

# Peroxo and superoxo anions: A DFT study on Fe/ZSM-5 zeolite

Gang Yang <sup>\*,1</sup>, Lijun Zhou <sup>1</sup>, Xianchun Liu, Xiuwen Han, Xinhe Bao <sup>\*</sup>

*State Key Laboratory of Catalysis, Dalian Institute of Chemical Physics, Chinese Academy of Sciences, Dalian 116023, PR China*

Received 15 January 2007; accepted 12 March 2007

Available online 21 March 2007

## Abstract

Metal peroxide species are the active sites in lots of solid-state and enzyme catalytic systems. With density functional calculations, the configurations of peroxide and superoxide anions in Fe/ZSM-5 zeolite were first resolved. The presence of superoxide anion was validated, which is less stabilized than the peroxide anion, especially at higher temperatures. It acts as the precursor to the active peroxide anion. Raman frequencies of these two species were analyzed considering <sup>18</sup>O/<sup>16</sup>O isotope effects. The present results are in fine agreement with previous theoretical and experimental results.

© 2007 Elsevier B.V. All rights reserved.

*Keywords:* Active site; Density functional; Peroxide; Superoxide; Fe/ZSM-5 zeolite

## 1. Introduction

Phenol and methanol constitute two important intermediates in today's chemical industries. However, several problems and drawbacks are currently present in the related manufacturing processes. Taking phenol as example, it is heavily dependent on the market demand of acetone, since they were co-produced in 1:1 ratio through the conventional three-step process via cumene. Fe/ZSM-5 zeolite seems to be a potential catalyst for replacing the tedious and energy-costing process, thus evolving into a research focus [1]. When treated with the oxidant N<sub>2</sub>O, the Fe/ZSM-5 catalyst generates the so-called “ $\alpha$ -oxygen” at the iron sites [2], which can be selectively inserted into the C–H bonds. Accordingly, the oxidation of benzene into phenol is completed within a single step.

Up to date, no agreement has been reached as to the nature of active sites in Fe/ZSM-5 zeolite. Analogous to the enzymatic system of methane monooxygenase

(MMO), the hydroxylation process catalyzed by Fe/ZSM-5 zeolite can proceed at quite low temperatures. Many characterization techniques such as <sup>27</sup>Al MAS NMR, CO-TPR, ESR, EXAFS, FT-IR, and Mössbauer [2–5] detected the binuclear, oxygen-bridged iron species present in Fe/ZSM-5 zeolite, which much resemble the active sites in MMO. Besides the single bridging oxygen species [6,7], two bridging oxygen species such as superoxide (O<sub>2</sub><sup>-</sup>) and peroxide (O<sub>2</sub><sup>2-</sup>) ions have been implicated to be the possible forms of adsorbed oxygen. The ESR experiments evidenced the formation of superoxide ions in Fe/ZSM-5 zeolite at 77 K [3,8]. At the temperature goes up, the superoxide ions are likely to convert into the peroxide ions, which become silent in the ESR spectra but active in the Raman spectra [9,10].

Recently, Prof. C. Li has given a report related with Fe/ZSM-5 zeolite, concluding that with the aid of UV-Raman technique, they also observed the presence of peroxo anion in Fe/ZSM-5 zeolite; however, they and their collaborators failed to obtain its configuration. The peroxide anion was also found in other metal-exchanged zeolites; e.g., Co/ZSM-5 [3,8]. In metal oxide systems such as La<sub>2</sub>O<sub>3</sub> and Ba/MgO, the peroxide ions are closely involved in the catalytic processes of nitric oxide decomposition and methane oxidation [11,12]. Owing to the presence of superoxide and

<sup>\*</sup> Corresponding authors. Fax: +86 0451 82102082 (G. Yang).

E-mail addresses: [dblyyg@nefu.edu.cn](mailto:dblyyg@nefu.edu.cn) (G. Yang), [xhbao@dicp.ac.cn](mailto:xhbao@dicp.ac.cn) (X. Bao).

<sup>1</sup> Present address: Key Laboratory of Forest Plant Ecology, Northeast Forestry University, Ministry of Education, Harbin 150040, PR China.

peroxide ions, the zeolite-like  $\text{Ca}_{12}\text{Al}_{10}\text{Si}_4\text{O}_{35}$  exhibits high activity for the oxidation of hydrocarbons [13]. The symmetric superoxide ions are likely to be present in enzyme MMO when activated by oxygen [14]. As indicated in Ref. [15], the active peroxide ions were converted from an unknown metastable compound. Therefore, it is of high value to investigate the structures of superoxide and peroxide species. Raman frequencies were also performed and analyzed for these two species, considering the  $^{18}\text{O}/^{16}\text{O}$  isotope effect. To understand the catalytic processes, the interconversion between superoxide and peroxide species was also discussed, meanwhile resolving the unknown metastable compound mentioned above.

## 2. Computational details

The local ZSM-5 structures were represented by 5 T clusters, with the Al atom occupying one of the T12 sites, see Fig. 1. The present clusters have been used in our previous work [7,16], which are slightly larger than the usually adopted ones [17] by replacing six terminal Si–H groups with Si–OH groups. In order to remain the local structure of ZSM-5 zeolite, the boundary Si and O atoms were fixed in their crystallographic positions.

First principle density functional calculations were performed under Gaussian98 program [18], using B3LYP functional. All the atoms except Fe were modelled with the commonly used 6-31G(d) basis. As to the element of Fe, its core electrons were represented by LANL2DZ effective core potential, and the valence electrons were described by LANL2DZ basis supplemented with one f-function [16]. The Fe atoms were considered at high-spin (sextet) states.  $\langle S^2 \rangle$  values were computed for all the cluster models, confirming that the spin contaminations are neglectable.

## 3. Results and discussion

The H/ZSM-5 zeolite cluster was depicted in Fig. 1, where the bridging H–O<sub>36</sub> distance was optimized at

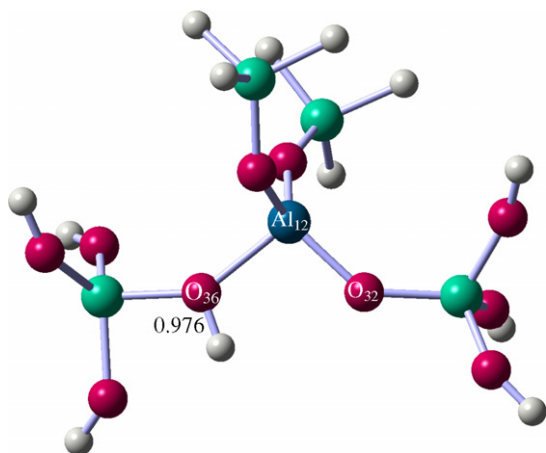


Fig. 1. The H-form ZSM-5 zeolite cluster.

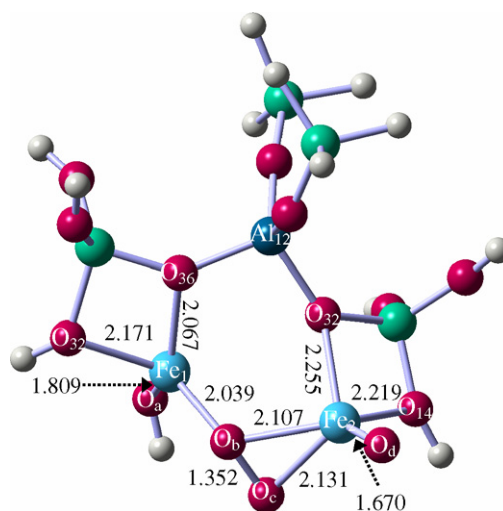


Fig. 2. Iron superoxide species in Fe/ZSM-5 zeolite ( $^1\text{Conf}$ ).

0.976 Å. The value is close to those of 0.969–0.980 Å obtained at BLYP/DNP and B3LYP/6-31G(d,p) theoretical levels [19]. The Brønsted acidic proton can be exchanged by the binuclear Fe species, see Fig. 2 ( $^1\text{Conf}$ ) and Fig. 3 ( $^2\text{Conf}$ ). The coordination environments of the Fe<sub>1</sub> site are similar in  $^1\text{Conf}$  and  $^2\text{Conf}$ , which is also applicable to the Fe<sub>2</sub> site. The Fe<sub>1</sub> site forms direct bonds with two lattice O atoms (O<sub>32</sub> and O<sub>36</sub>) with the distances at ca. 2.1 Å, which is consistent with the previous theoretical and XAFS experimental data [6,7,17]. There are three extra-framework oxygen atoms (O<sub>a</sub>, O<sub>b</sub> and O<sub>c</sub>) around the Fe<sub>1</sub> site, among which the hydroxyl group displays the greatest interplay with the Fe<sub>1</sub> site as evidenced by the shortest Fe<sub>1</sub>–O distance at 1.809 Å. The interacting strength between O<sub>b</sub> and Fe<sub>1</sub> is comparable to that of lattice O atoms. The Fe<sub>1</sub>–O<sub>c</sub> distance was calculated to be 1.909 Å in  $^2\text{Conf}$  whereas 2.910 Å in  $^1\text{Conf}$ , suggesting direct Fe–O bonds formed in the former whereas only weak interactions present in the latter. It is the only difference in

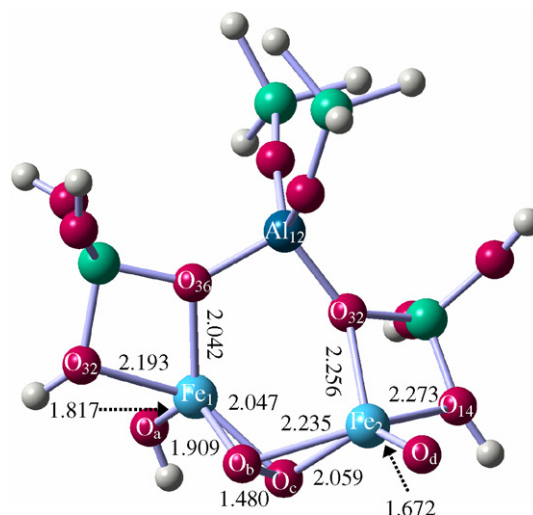


Fig. 3. Iron peroxide species in Fe/ZSM-5 zeolite ( $^2\text{Conf}$ ).

Table 1  
Superoxide and peroxide species

	O <sub>2</sub>	O <sub>2</sub> <sup>-</sup>	H <sub>2</sub> O <sub>2</sub>	O <sub>2</sub> <sup>-</sup> in <sup>1</sup> Conf	O <sub>2</sub> <sup>2-</sup> in <sup>2</sup> Conf
O–O distance, Å	1.215	1.353	1.456	1.352	1.480
Mulliken charge	0.000	-1.000	-2.000	-1.317	-1.981
Spin density	2.000	1.000	0.000	1.135	0.691
$\nu_{\text{O-O}}$ , cm <sup>-1</sup>	1509.4	1103.1	875	1007.3	807.4

the Fe<sub>1</sub> coordination environments of these two configurations (<sup>1</sup>Conf and <sup>2</sup>Conf). As to the Fe<sub>2</sub> site, it is also bonded to two lattice O atoms (O<sub>32</sub> and O<sub>14</sub>); however, their bonds are elongated by approximately 0.1 Å compared with those of the Fe<sub>1</sub> site. Analogous to the Fe<sub>1</sub> site, three extra-lattice O atoms (O<sub>b</sub>, O<sub>c</sub> and O<sub>d</sub>) are present nearby the Fe<sub>2</sub> site. The Fe–O<sub>d</sub> distance is equal to 1.67 Å characteristic of Fe=O double bond [6,7]. Unlike the Fe<sub>1</sub> site in <sup>1</sup>Conf, the Fe<sub>2</sub> sites in both configurations form direct bonds with two bridging O atoms, with the Fe<sub>2</sub>–O distances optimized at 2.107 and 2.131 Å in <sup>1</sup>Conf, and 2.059 and 2.235 Å in <sup>2</sup>Conf, respectively.

As aforementioned, the binuclear Fe species are connected by two bridging O atoms (O<sub>b</sub> and O<sub>c</sub>) in the Fe-exchanged ZSM-5 zeolite. The O<sub>b</sub>–O<sub>c</sub> distances were optimized at 1.352 Å in <sup>1</sup>Conf and 1.480 Å in <sup>2</sup>Conf, respectively. The oxygen molecule (O<sub>2</sub>), the superoxide anion (O<sub>2</sub><sup>-</sup>) and the hydrogen peroxide molecule was geometry-optimized under the same theoretical method as elucidated in the part of Computational details. The O–O distances in these three species were calculated to be 1.215, 1.353 and 1.456 Å (Table 1), respectively, indicating the gradual elongation of O–O distance as more negative charges were imposed. It can also be observed that the O–O distances in <sup>1</sup>Conf and <sup>2</sup>Conf are close to those in O<sub>2</sub><sup>-</sup> and H<sub>2</sub>O<sub>2</sub>, respectively. The Mulliken charges on the O<sub>2</sub><sup>x-</sup> ions (x = 1 or 2) in <sup>1</sup>Conf and <sup>2</sup>Conf were calculated at -1.317 and -1.981 |e| [20], which are also close to those in O<sub>2</sub><sup>-</sup> and H<sub>2</sub>O<sub>2</sub>, respectively. The two bridging O atoms (O<sub>b</sub> and O<sub>c</sub>) are neighboring to the high-spin Fe<sub>1</sub> and Fe<sub>2</sub> sites, and therefore it is inevitable to be spin contaminated and “share” some of the spin densities of the Fe sites. Accordingly, the spin densities on O<sub>b</sub> and O<sub>c</sub> will deviate from the presumed values (see Table 1). However, the changing tendency can still well represent that the O<sub>2</sub><sup>x-</sup> species in <sup>1</sup>Conf and <sup>2</sup>Conf are described as the superoxide (O<sub>2</sub><sup>-</sup>) and peroxide (O<sub>2</sub><sup>2-</sup>) ions respectively, combining the theoretical results of O–O distances and Mulliken charges on O<sub>2</sub><sup>x-</sup>.

The free O<sub>2</sub> molecule is inactive in Raman spectra; however, it has a theoretical value at 1509.4 cm<sup>-1</sup> [21], agreeing with the experimental value at 1556 cm<sup>-1</sup> for gas-phase and physisorbed O<sub>2</sub> species [10]. The  $\nu_{\text{O-O}}$  Raman frequencies were calculated to be 1007.3 and 807.4 cm<sup>-1</sup> in <sup>1</sup>Conf and <sup>2</sup>Conf, which are in good consistency with the experimental values within the range 1015–1180 cm<sup>-1</sup> [22] and around 800 cm<sup>-1</sup> [14], respectively. Gao et al. [10] ascribed the peak at 730 cm<sup>-1</sup> to the peroxide ions in Fe/ZSM-5 zeolite. According to our calculated Raman spectra, there

are at least 13 peaks within the range of 630–830 cm<sup>-1</sup>. Some are comparable, and the one at 778.2 cm<sup>-1</sup> is very intense and about 3.5 times as strong as that of the peroxide anion. The Raman peak at 778.2 cm<sup>-1</sup> was ascribed to the stretching mode of Fe=O<sub>d</sub> double bond, which is also closely related with the binuclear Fe species. Accordingly, it becomes very difficult to assign the experimental Raman spectra even with the aid of <sup>18</sup>O isotopes. The vibrations of O<sub>2</sub><sup>x-</sup> in Fe/ZSM-5 zeolite deviate much from those in O<sub>2</sub><sup>-</sup> and H<sub>2</sub>O<sub>2</sub> (Table 1), as a result of the interplays between the binuclear Fe site and zeolite framework. Moreover, the iron superoxide and peroxide species exert different influences although slightly on the zeolite frameworks. For example, one Si–O–Al stretching mode was computed to fall at 1012.3 and 1008.3 cm<sup>-1</sup> in <sup>1</sup>Conf and <sup>2</sup>Conf, respectively. <sup>18</sup>O isotope effects were also considered in the present Raman spectral calculations, and O<sup>18</sup>–O<sup>18</sup> vibrates at 949.6 and 763.8 cm<sup>-1</sup> in <sup>1</sup>Conf and <sup>2</sup>Conf, respectively. According to our theoretical results, the red shifts due to the O<sup>18</sup> isotope effects equal 57.7 and 43.6 cm<sup>-1</sup> for the superoxide and peroxide species, respectively. The values are in good agreement with those obtained from the reduced mass, at 57.0 and 45.7 cm<sup>-1</sup>, respectively.

At 298.15 K and 1 atm, <sup>1</sup>Conf is less stable compared to <sup>2</sup>Conf with the energy difference ( $E_{\text{diff}}$ ) calculated to be 6.1 kJ mol<sup>-1</sup>. Corrected with the zero-point energy (ZPE), the energy difference amounts to 8.0 kJ mol<sup>-1</sup>. The energy difference ( $E_{\text{diff}}$ ) at other temperatures can be estimated with the inclusion of thermal corrections. At lower temperatures such as 77 K in Refs. [3,8,9], the energy difference ( $E_{\text{diff}}$ ) was obtained to be around 5.0 kJ mol<sup>-1</sup>. It suggests that in comparison with the iron peroxide anion, the superoxide anion is relatively more stable at lower temperatures. As the temperature or the reaction time increases, the superoxide ions will be gradually converted into the more stable peroxide ions, in perfect agreement with the previous experimental results [9]. Therefore, the unknown metastable species pointed out in Ref. [14] should be attributed to the superoxide species, which acts as the precursor to the active peroxide anion during catalytic processes [15].

#### Acknowledgements

We gratefully acknowledged the financial support (2003CB615806) from the National Natural Science Found-

dition and the Ministry of Science and Technology of the Peoples' Republic of China.

## References

- [1] G.I. Panov, *Cattech* 4 (2000) 18.
- [2] K.A. Dubkov, N.S. Ovanesyan, A.A. Shteinman, E.V. Starokon, G.I. Panov, *J. Catal.* 207 (2002) 341.
- [3] H.Y. Chen, El-M. El-Malki, X. Wang, W.M.H. Sachtler, *J. Mol. Catal. A: Chem.* 162 (2000) 159.
- [4] P. Marturano, L. Drozdová, A. Kogelbauer, R. Prins, *J. Catal.* 192 (2000) 236.
- [5] A.A. Battiston, J.H. Bitter, F.M.F. de Groot, A.R. Overweg, O. Stephan, J.A. van Bokhoven, P.J. Kooyman, C. van der Spek, G. Vankó, D.C. Koningsberger, *J. Catal.* 213 (2003) 251.
- [6] A.L. Yakovlev, G.M. Zhidomirov, R.A. van Santen, *J. Phys. Chem. B* 105 (2001) 12297.
- [7] G. Yang, D.H. Zhou, X.C. Liu, X.W. Han, X.H. Bao, *J. Mol. Struct.* 797 (2006) 131.
- [8] El-M. El-Malki, D. Werst, P.E. Doan, W.M.H. Sachtler, *J. Phys. Chem. B* 104 (2000) 5924.
- [9] F.A. Cotton, G. Wilkinson, C.A. Murillo, M. Bochmann, *Advanced Inorganic Chemistry*, sixth ed., John Wiley & Sons, New York, 1999, pp. 465–471.
- [10] Z.X. Gao, H.S. Kim, Q. Sun, P.C. Stair, W.M.H. Sachtler, *J. Phys. Chem. B* 105 (2001) 6186.
- [11] S. Xie, G. Mestl, M.P. Rosynek, J.H. Lunsford, *J. Am. Chem. Soc.* 119 (1997) 10186.
- [12] G. Mestl, M.P. Rosynek, J.H. Lunsford, *J. Phys. Chem. B* 102 (1998) 154.
- [13] S. Fujita, K. Suzuki, M. Ohkawa, T. Mori, Y. Iida, Y. Miwa, H. Masuda, S. Shimada, *Chem. Mater.* 15 (2003) 255.
- [14] L. Que Jr., Y.H. Dong, *Acc. Chem. Res.* 29 (1996) 190, and references cited therein.
- [15] E.I. Solomon, T.C. Brunold, M.I. Davis, J.N. Kemsley, S.K. Lee, N. Lehnert, F. Neese, A.J. Skulan, Y.S. Yang, J. Zhou, *Chem. Rev.* 100 (2000) 235, and references cited therein.
- [16] G. Yang, L.J. Zhou, X.C. Liu, X.W. Han, X.H. Bao, *J. Phys. Chem. B* 110 (2006) 22295.
- [17] J.A. Ryder, A.K. Chakraborty, A.T. Bell, *J. Catal.* 220 (2003) 84.
- [18] M.J. Frisch, G.W. Trucks, H.B. Schlegel, G.E. Scuseria, M.A. Robb, J.R. Cheeseman, V.G. Zakrzewski, J.A. Montgomery Jr., R.E. Stratmann, J.C. Burant, S. Dapprich, J.M. Millam, A.D. Daniels, K.N. Kudin, M.C. Strain, O. Farkas, J. Tomasi, V. Barone, M. Cossi, R. Cammi, B. Mennucci, C. Pomelli, C. Adamo, S. Clifford, J. Ochterski, G.A. Petersson, P.Y. Ayala, Q. Cui, K. Morokuma, D.K. Malick, A.D. Rabuck, K. Raghavachari, J.B. Foresman, J. Cioslowski, J.V. Ortiz, A.G. Baboul, B.B. Stefanov, G. Liu, A. Liashenko, P. Piskorz, I. Komaromi, R. Gomperts, R.L. Martin, D.J. Fox, T. Keith, M.A. Al-Laham, C.Y. Peng, A. Nanayakkara, C. Gonzalez, M. Challacombe, P.M.W. Gill, B. Johnson, W. Chen, M.W. Wong, J.L. Andres, C. Gonzalez, M. Head-Gordon, E.S. Replogle, J.A. Pople, *Gaussian 98*, Revision A.9, Gaussian, Inc., Pittsburgh, PA, 1998.
- [19] G. Yang, X.C. Liu, X.W. Han, X.H. Bao, *J. Phys. Chem. B* 110 (2006) 23388.
- [20] The Mulliken charge on the  $O_2^{2-}$  species in  $H_2O_2$  was calculated to be  $-0.835 |e|$ , which was multiplied to  $-2.000 |e|$  with a scaling factor of 2.395. The same scaling factor was applied to the  $O_2^{x-}$  species in  $^1Conf$  and  $^1Conf$ .
- [21] The  $\nu_{O-O}$  frequencies in  $H_2O_2$  fall at 875 and  $957.31 \text{ cm}^{-1}$  at the experimental and B3LYP/6-31 G(d) theoretical levels, respectively. By comparing these two values, a scaling factor of 0.91 was reached for the present work.
- [22] M. Che, A.J. Tench, *Adv. Catal.* 32 (1983) 1.